20th Australasian Fluid Mechanics Conference
Perth, Australia
5-8 December 2016

High Resolution Simulation of Dissolution Process under Sloping Ice-shelves in Saline Water

Mainak Mondal[1], Bishakhdatta Gayen[1], Ross W. Griffiths[1] and Ross C. Kerr[1]

[1]GFD, Research School of Earth Sciences
Australian National University, Canberra, ACT 2601, Australia

Abstract

Direct Numerical Simulation is performed to study the dissolution/melting process of sloping ice-shelves at fixed ambient salinity and temperature. A series of numerical simulations are carried out over various inclinations of the ice block with the horizontal direction. Both laminar and turbulent flows are simulated over shallower slopes. When the boundary layer is laminar, dissolution-rate varies along the slope-length, which decreases in the upslope direction. Dissolution rate is independent in the upslope direction when the boundary layer becomes turbulent. These results are geophysically relevant and can be developed further towards a better parametrisation scheme for the GCMs to estimate the ice-loss around Antarctica.

Introduction

The melting of the polar ice is a threat to the global climate. Fresh-water flux from the melt ice is influencing the thermohaline circulation [3], causing the redistribution of temperature and rainfall patterns across the globe, while loss of ice cover [2] is creating a positive feed back to the total radiation budget, thus directly influencing the global warming. Finally the loss of land ice is causing the sea level to rise. The overall Antarctic ice-loss is increased by 75% [1] in past decades. The warm and salty Circumpolar Deep Water is entering into the ice-shelf cavities at Antarctica and melting ice by turbulent transport of salt and heat at the ice-ocean interface [1].

Present Global Climate Models (GCM) work at scales O(1-100 km), therefore they are unable to resolve convections close to the ice-walls and rely on parameterisation schemes. Since the simulated melt rates from these models are very much sensitive to the parameterisation schemes, they need to be tested thoroughly while the effects of convection need to be incorporated to obtain better estimation of ice-loss rates. A pioneering experimental and theoretical work had been done by Josberger and Martin [4], who found the scaling law for ablation rate based on turbulent diffusivities of heat and salt. Woods [7] Kerr [**?**]distinguished this diffusion governed dissolution of ice, from melting suggested that the dissolution can occur even when the temperature of the ambient salt water is lower than the melting temperature. Based on experimental data, Kerr & McConnochie [6] derived necessary scalings for dissolution of vertical ice blocks with a turbulent boundary layer. Recently, Gayen et al., [5] have taken a numerical approach to this small scale phenomena using Direct Numerical simulations (DNS). The flow field is fully resolved and thermal and saline boundary layers are estimated. The simulated dissolution rates agree very well with the experimental data over the spectrum of ambient temperature ($-1^\circ - 6^\circ$C) and salinity ($10 - 35$ psu). This leaves a new pathway of ice-loss modelling in a regional scale, resolving small scale turbulence.

However, observations reveal that most of the fast-decaying ice-shelves are not vertical, rather inclined forward into the sea due to a higher loss at the bottom part. Under these sloping ice-shelves the flow field close to the ice-wall becomes complex. The buoyancy acts both in slope parallel and wall normal direction, that influences the transfer of heat through the ice-ocean interface and hence the ice-loss rate. In the present work we use DNS to study the effects of slope on the boundary layer processes and the resultant dissolution rate. Slope angles are varied from vertical to near horizontal. Turbulent flow field for these shallower slopes is simulated with proper choice of domain length.

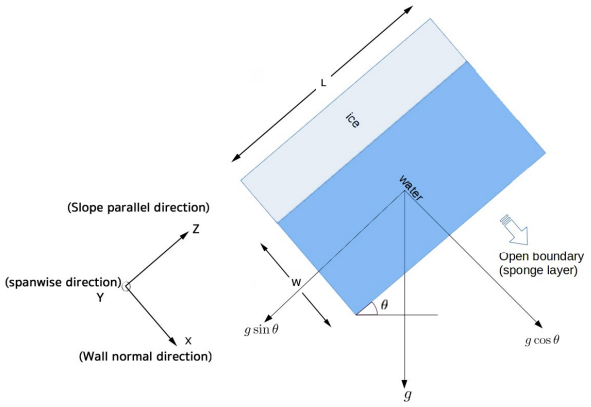

Figure 1: Configuration of the domain

Formulation of the problem and solution techniques

The flow is simulated in a rectangular box with length L, width W and depth D. The Z, X and Y directions are the slope parallel, wall normal and span-wise directions respectively (figure 1). The longer edge on the left hand side of the domain serves the necessary interface conditions of a virtual ice wall aligning with the slope. Depending on the slope angle the domain is rotated to match the above arrangements while gravity is always acting in downward direction. Flow velocities in the Z, X and Y directions are represented by w, u and v respectively. The saline water has kinematic viscosity ν, molecular, thermal and saline diffusivities, κ_T and κ_S, coefficient of thermal expansion α_T and coefficient of haline contraction γ_S. The continuity, momentum and flux balance equations can be written as follows:

$$\nabla \cdot \vec{\mathbf{u}} = 0$$

$$\partial u/\partial t + (\vec{u}.\vec{\nabla})u = -\frac{1}{\rho_0}\frac{\partial p^*}{\partial x} + \nu\nabla^2 u + \frac{\rho^*}{\rho_0} g\cos\theta$$

$$\partial w/\partial t + (\vec{u}.\vec{\nabla})w = -\frac{1}{\rho_0}\frac{\partial p^*}{\partial z} + \nu\nabla^2 w - \frac{\rho^*}{\rho_0} g\sin\theta$$

$$\partial v/\partial t + (\vec{u}.\vec{\nabla})v = -\frac{1}{\rho_0}\frac{\partial p^*}{\partial y} + \nu\nabla^2 v$$

$$\partial T^*/\partial t + (\vec{u}.\vec{\nabla})T^* = \kappa_T \nabla^2 T^*$$

$$\partial S^*/\partial t + (\vec{u}.\vec{\nabla})S^* = \kappa_T \nabla^2 S^*$$

$$\rho^* = \rho_0(\gamma_S S^* - \alpha_T T^*)(1)$$

Here $p^*, T^*, S^*$and ρ^* denote deviation from the background hydrostatic pressure (p_b), temperature (T_W), salinity (S_W) and density (ρ_0), respectively. To study the predominant effect of slope on the melting/dissolving process, certain internal parameters are required to be fixed. They are Grashof number (Gr), Prandtl number (Pr), Schmidt number (Sc) and Stefan's number(Se) respectively. Mathematically they are defined as follows:

$$Gr \equiv \frac{\gamma_S g(S_w - S_i)L^3}{\nu^2}, Pr \equiv \frac{\nu}{\kappa_T}, Sc \equiv \frac{\nu}{\kappa_S}, Ste \equiv \frac{\rho_w C_w (T_W - T_i)}{\rho_s Ł}, \tag{2}$$

Where T_i, S_i are the interface and T_W, S_W are the far field temperature and salinity respectively. C_w is the specific heat, ρ_W and ρ_S are the densities of fresh and saline water and Ł is the latent heat of saline water. For simulations with different slopes we choose sine of the slope angle, $\sin\theta$ as another external parameter.

Along with Navier-Stokes (NS) equations the other fundamental equations for this problem are freezing point depression equation and flux conservation equations for heat and salt respectively. The freezing point of saline water is assumed to be a linear function of salinity and pressure. For our numerical simulations, the effect of pressure is neglected due to small domain size and interface temperature is represented as

$$T_i = a_S S_i + bP_i \simeq a_S S_i, \tag{3}$$

where Si is the salinity at the interface. For antarctic conditions the value of a_s is fixed at -6×10^{-2}°C/psu. The second equation expresses the balance between latent heat flux Q_m^H, due to dissolution, with the divergence of heat at the interface into ice and water. It is expressed as,

$$Q_{ice}^H - Q_w^H = Q_m^H. \tag{4}$$

Here Q_{ice}^H and Q_w^H are the heat fluxes to the interface in the ice and water, respectively. Owing to the low conductivity of ice we neglect the heat transfer through the ice surface ($Q_{ice}^H \sim 0$). Hence above equation can be written as,

$$-\rho_w C_p \kappa_T \frac{\partial T}{\partial x}|_{x=0}^A = \rho_S V Ł A_i. \tag{5}$$

Here V is the dissolution velocity, C_P is the specific heat of ambient water and A_i is the contact area between ice and water. Analogous equation is used to describe the salt flux balance as a result of fresh water release and salt flux divergence at the interface due to dissolution, given as,

$$Q_{ice}^S - Q_w^S = Q_m^S. \tag{6}$$

The diffusivity of salt through ice is much less compared to that of water, Q_{ice}^S can therefore be neglected for convenience of calculation. Above equation, can therefore be written as

$$-\rho_w \kappa_S \frac{\partial S}{\partial x}|_{x=0}^A = \rho_S S_i V A_i. \tag{7}$$

Using equation 3, 5 and 7 the interface conditions for the simulation can be determined.

In order to ensure turbulence in the present study, laminar to turbulent transition length (L_t) for different slope angles is theoretically estimated based on critical Grashof number, Gr_C. L_t can be expressed as,

$$L_t = \left(\frac{\nu^2 Gr_C}{g \sin\theta \gamma_S (S_w - S_i)}\right)^{\frac{1}{3}}. \tag{8}$$

The typical values of Gr_C lie in between $10^9 - 10^{10}$. Based on this calculation, for the angle range 50° to 90°, turbulent flows can be simulated within 1m of slope length of the respective domains (figure 2). However for shallower angles which are 20° or below, L_t are found to be over 2m. Therefore two domains are considered of length of 1.8 m for angle range $50° - 90°$, and 20 m for angles $5° - 20°$, to ensure domain length is well above transition. Accordingly in our simulation we have used a Gr of 7.5×10^{11} for the smaller domain and 10.28×10^{14} for the longer domain, while Pr of 14 and Sc of 2500 are kept same for both domains. The far field temperature $T_w = 2.3°$ C and salinity $S_w = 35$ psu are remained fixed for all cases.

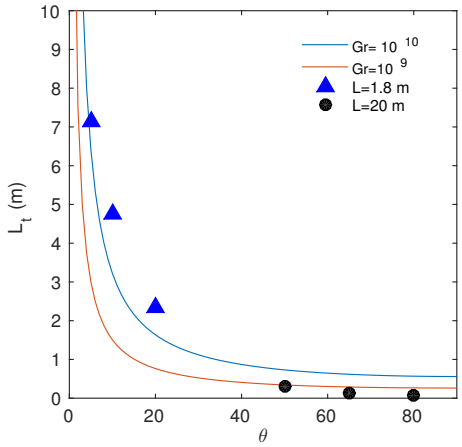

Figure 2: Theoretical laminar to turbulent transition length, L_t (solid-lines) based on the critical Gr_C band $10^9 - 10^{10}$ along with the numerically simulated values (points), based on the distance from bottom. Here L_t is calculated along the slope-length, where tke, integrated over wall normal direction reaches 18% of it's maximum value over the domain.

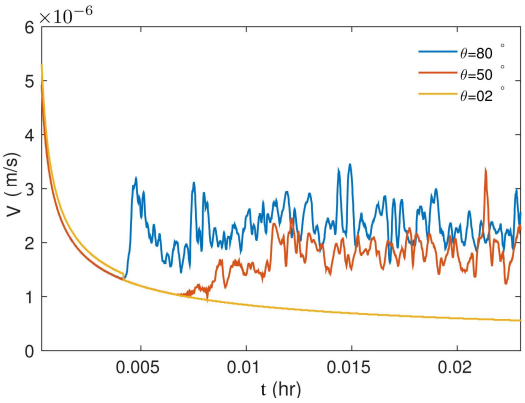

Figure 3: Temporal evolution of dissolution rate, $|V|$ (m/s), measured at mid-length for 1.8 m domain with $\theta = 80°$, 50° and 2° respectively.

Results

All simulations start with uniform temperature and salinity

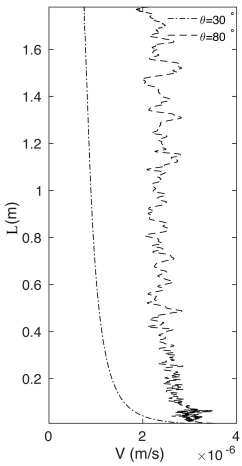

Figure 4: Along slope profile of dissolution rate, $|V|$ (m/s) calculated as wall normal velocity at the interface, for $L = 1.8$ m and $\theta = 30^\circ$ and 80°, respectively.

which are equal to the far field values. White noise is imposed in the velocity field concentrated near the interface with zero mean velocity. We have plotted the temporal evolution of simulated dissolution rates, measured at the interface with 1.8m domain for 80°, 65° and 10° slope angles respectively, as shown in figure 3. Due to formation of boundary layer against the interface, the initial dissolution rate is found to be much higher and it slows down rapidly to a quasi steady state. The duration of this transition to quasi steady state increases with shallower angles, 0.00042 hrs for 80° slope to 0.02044 hrs for 2° slope in 1.8 m domain (figure 3). In the quasi-steady state the steeper angle ($\theta = 80^\circ$) shows high frequency variability both in dissolution rate and interface temperature (not shown here) than compared to $\theta = 2^\circ$ slope where the boundary layer is laminar.

The along slope profile of simulated dissolution rates show distinct features for laminar and turbulent flows inside the boundary layers. In figure 4, it is observed that for $\theta = 30^\circ$, where flows field is laminar, the dissolution rate decreases along the slope-length. However, for turbulent flow field with $\theta = 80^\circ$ such trend can not be found and the dissolution rate is independent of slope length. The overall magnitudes of the dissolution rates are also less for the shallower slope angle. The simulated dissolution rates at mid-length of the domain (figure 5) are plotted against slope angles. The dissolution rate decreases from 2.44 μm for 90° slope to 0.3120 μm for 5° slope. Dissolution rate over slope angles has shown different trends depending on whether the flow is laminar or turbulent. All the laminar dissolution rates are measured at mid-lengths of the 1.8 m domain. The dissolution rate for laminar flows decreases more gradually compared to the turbulent flows.

The snapshots of the slope parallel velocities for L= 1.8 m and L= 20 m are shown in figure 6 and 7, respectively. Contact of the ice with the salt water at ambient conditions causes the release of buoyant melt water with low salinity in the vicinity of the interface, forming a very thin fresher boundary layer. At the same time due to cooling from the ice surface, a thermal boundary layer is created that extends far beyond the inner boundary layer. For steeper angles a bidirectional flow is visible at the lower part of the simulation domain (figure 6 (b)) where upward flow due to freshening is observed right adjacent to the ice wall, and on the outer side, a wider downward flow is observed following gravity direction as a result of cooling. The along-

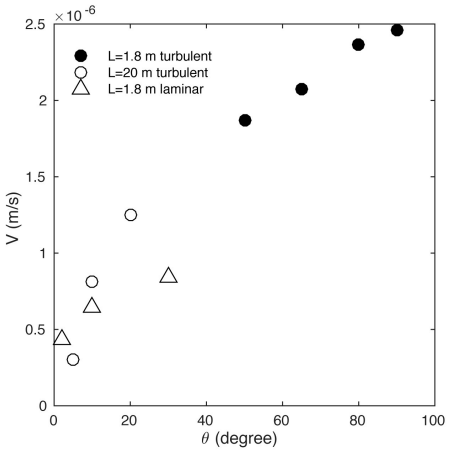

Figure 5: Variation of dissolution rate, $|V|$ (m/s) with slope angle θ, plotted at $T_W = 2.3^\circ$ and $S_W = 35$ psu.

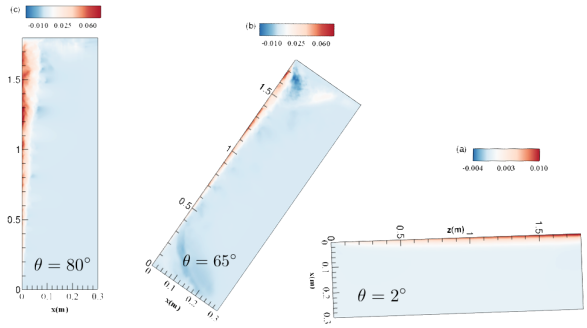

Figure 6: Snapshots for along slope velocity field (w) in (m/s) over $\theta = 80^\circ$, 65° and 2° respectively for L= 1.8 m.

slope flow accelerates as it moves upslope and at the same time spreads in wall normal direction due to entrainment from quiescent surrounding fluid. With the shallower angles this flow becomes weaker and fluctuations in the flow-field completely disappears for $\theta \leq 30^\circ$ in the smaller domain. The wall normal buoyancy in the outer layer prevents the wall normal spreads of the buoyant plume.

Figure 7 shows the along-slope flow field at angles, $\theta = 20^\circ$, 10° and 5° where variability in the flow-fields is observed. With shallower slopes, the along-slope buoyancy becomes weaker. Therefore the flow has to traverse longer to be strong enough to create turbulent fluctuations. For all the cases with L= 20 m, patches of variability can be seen at regular intervals up to mid-length of the domain where the flow is still undergoing laminar to turbulent transition. The variability becomes consistent for slope length over 15 m where it has grown into a fully-turbulent flow.

Conclusions

This study incorporates the effects of slope on the dissolution rates at ambient conditions as found in the Antarctic basins. These simulations capture evolution of flow field at the dissolving ice shelves over the geophysical range of slope angles. The simulated dissolution rates with longer domain have revealed that they are independent of the domain length and hence the *Gr*, and is mostly dependent on the slopes of the ice blocks. It has been found that the dissolution rate decreases with shallower slope angles from 2.44 μm/s for the vertical wall

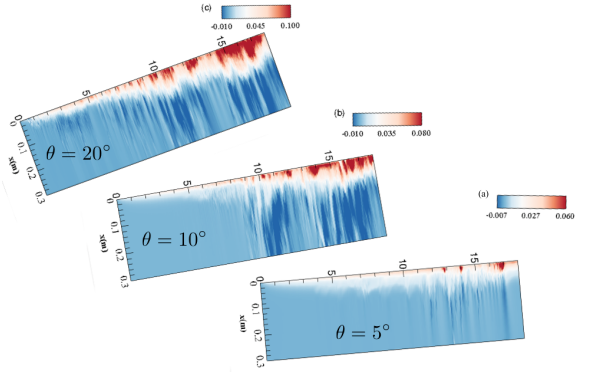

Figure 7: Similar figure as above but with $\theta = 20°, 10°$ and $5°$ respectively with L= 20 m. The flow features are stretched along the wall-normal direction to mach the aspect ratio.

to 0.3120 μm/s for the shallowest case with slope angle $\theta = 5°$. Most importantly we are able to simulate turbulent flows in a slope as shallow as $\theta = 5°$, where the flow is still buoyancy driven. Investigation of the slope dependency of the thermal and saline boundary layer thicknesses is under process and we hope that it would reveal a better understanding once the results will be analysed.

References

[1] A. J. Payne, A. Vieli, A. P. Shepherd, D. J. Wingham and E. Rignot, Recent dramatic thinning of largest West Antarctic ice stream triggered by oceans., *Geophys. Res. Lett.*, 31, 2004, L23401.

[2] V. Laine, Antarctic ice-albedo temperature and sea ice concentration trends, 1981-2000. Finnish Meteorological Institute, PO Box 503, 00101, Helsinki, Finland, 2008.

[3] C. Lavergne, J. B. Palter, E.c D. Galbraith, R. Bernardello and I. Marinov, Cessation of deep convection in the open Southern Ocean under anthropogenic climate change., *Nature Climate Change*, 10.1038/NCLIMATE2132, 2014.

[4] E. G. Josberger and S. Martin, A laboratory and theoretical study of the boundary layer adjacent to a vertical melting ice wall in salt water *J. Fluid Mech*, vol: 111, 1981, 439-473.

[5] B. Gayen, R. W. Griffiths, R. C. Kerr, Simulation of convection at a vertical ice face dissolving into saline water., *J. Fluid Mech* , vol: 798, 2016, 284-298.

[6] R. C. Kerr and C. D. McConnochie, Dissolution of a vertical solid surface by turbulent compositional convectio., *J. Fluid Mech.*, vol: 765, 2015, 211-228.

[7] A. W. Woods, Melting and dissolving., *J. Fluid Mech.*, vol: 239, 1992, 429-448.

[8] R C. Kerr, Dissolving driven by vigorous compositional convection., *J. Fluid Mech*, vol: 280, 1994b, 287-302.